






Theoretical study of the $I^+ + I^-$ mutual neutralization reaction

Sylvain Badin ^{1,2} Xiang Yuan ^{1,3} Pierre-Louis Bourgeois ²
 Andre Severo Pereira Gomes ¹ and Nicolas Sisourat ^{2,*}

¹Univ. Lille, CNRS, UMR 8523-PhLAM-Physique des Lasers Atomes et Molécules, F-59000 Lille, France

²Sorbonne Université, CNRS, Laboratoire de Chimie Physique Matière et Rayonnement, UMR 7614, F-75005 Paris, France

³Department of Chemistry and Pharmaceutical Science, Faculty of Science, Vrije Universiteit Amsterdam, de Boelelaan 1083, 1081 HV Amsterdam, The Netherlands



(Received 8 November 2022; accepted 25 January 2023; published 13 February 2023)

We have computed the cross sections of the mutual neutralization reaction between I^+ and I^- for a collision energy varying from 0.001 eV to 50 eV. These cross sections were obtained using the adiabatic potential energy curves of the I_2 system computed with a direct relativistic multireference configuration interaction method and a semiclassical approach (i.e., Landau-Zener surface hopping). We report the cross sections towards the following neutral states: $I(^2P_{3/2}) + I(^2P_{3/2})$, $I(^2P_{3/2}) + I(^2P_{1/2})$, $I(^2P_{1/2}) + I(^2P_{1/2})$, and $I(5p^46s) + I(^2P_{3/2})$. We also discuss the cross sections towards the following two excited ionic states: $I^-(^1S_0) + I^+(^3P_0)$ and $I^-(^1S_0) + I^+(^3D_2)$. The results of these calculations are in qualitative accordance with recent experimental measurements conducted in the Double ElectroStatic Ion Ring ExpEriment (DESIREE) in Stockholm. These results can be used to model iodine plasma kinetics and thus to improve our understanding of the latter.

DOI: [10.1103/PhysRevA.107.022808](https://doi.org/10.1103/PhysRevA.107.022808)

I. INTRODUCTION

The mutual neutralization (MN) of two oppositely charged ions is a central reaction taking place in electronegative plasmas. The latter are found in, e.g., the lower ionosphere [1], flames [2], interstellar medium [3,4], and in excimer lasers [5]. As such, MN reactions have been investigated in various systems (see, e.g., Ref. [6] and references therein).

Iodine plasma is one example of an electronegative plasma. Interest in iodine plasma has been renewed recently since it is a promising candidate to be used in electric propulsion systems, notably for satellites (see, e.g., Refs. [7,8] and references therein).

Very recently, the MN reaction between I^+ and I^- ions has been studied experimentally by Poline *et al.* [9] at the Double ElectroStatic Ion Ring ExpEriment (DESIREE) facility: the branching ratios for the different channels were measured at two collision energies, 0.1 eV and 0.8 eV. This work showed that the MN reaction forms iodine atoms either in their ground state or with one atom in an electronically excited state. These two classes of states were found to be populated with nearly equal proportions with no dependence on the collision energy. The total cross sections at these collision energies were estimated, but with fairly large uncertainties.

There are currently no accurate absolute cross sections published for the MN reaction between I^+ and I^- ions, which impedes the modeling of iodine plasma. Investigating such a collision system is a difficult task since iodine has a strong spin-orbit coupling, and moreover, the potential energy curves of I_2 exhibit multiple and overlapping avoided crossings, where the MN reaction can take place. The aim of

the present work is to provide estimates of these cross sections in a broad range of collision energies. For that, we have employed a combination of *ab initio* relativistic electronic structure calculations and the Landau-Zener surface hopping (LZSH) method to compute the relevant cross sections. Our calculations are then compared to the recent experiments of Poline *et al.* [9].

This paper is organized as follows. In the next section we briefly outline the methods used in the present work. Section III is devoted to the discussion of the theoretical results of this work and their comparison with the experimental results obtained recently by Poline *et al.* [9] at the DESIREE double ion ring. The conclusions are reported in Sec. IV. Atomic units are used throughout, unless explicitly indicated otherwise.

II. METHODS

A. Potential energy curves

The potential energy curves used in this work, shown in Fig. 1, were already presented in Poline *et al.* [9]. They have been obtained with the multireference configuration interaction (MRCI) method, as implemented in the Kramers restricted configuration interaction (KRCI) module [10] of the DIRAC relativistic electronic structure package [11]. Such calculations have been carried out with the DIRAC19 [12] release as well as with the development version identified by hash 1e798e5. We employed triple-zeta quality basis sets [13] supplemented by diffuse functions so that Rydberg and ion-pair (IPr) states could be accurately represented. The exponents for the diffuse functions (listed in Table III of the Appendix) were automatically generated by DIRAC as even-tempered sequences based on the most diffuse exponents of the dyall.v3z basis. The reference wave function consisted of the set of

*Nicolas.sisourat@sorbonne-universite.fr

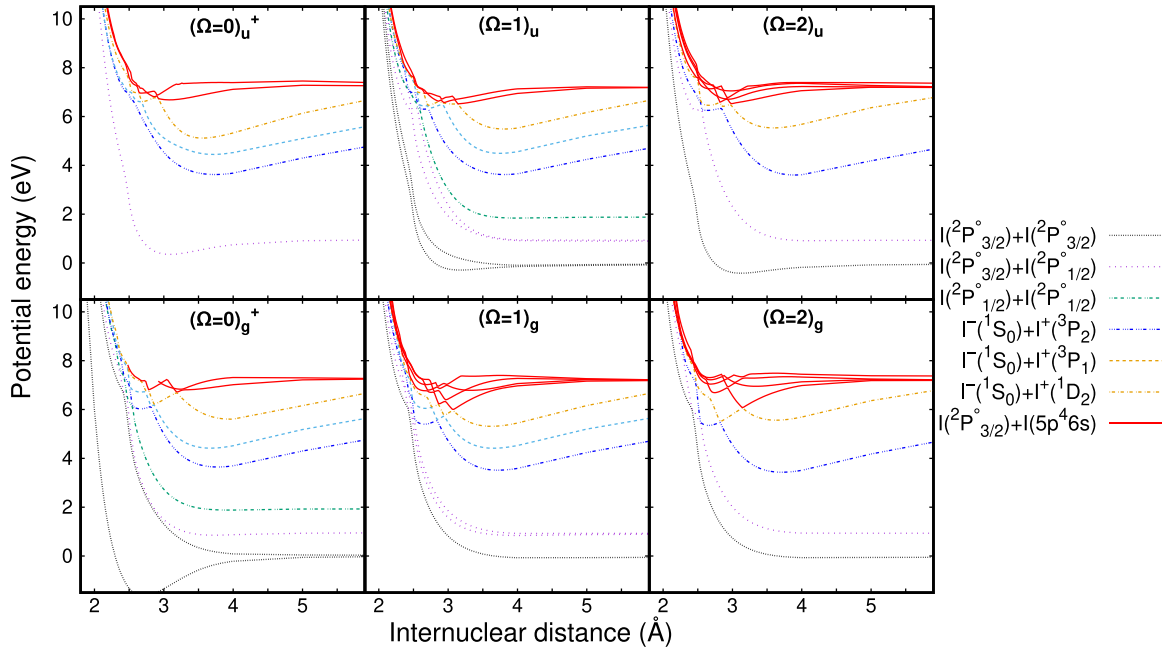


FIG. 1. Potential energy curves of 51 electronic states of I_2 computed with relativistic MRCI (reconstructed from the data from Poline *et al.* [9]). Only the states of the symmetries that correlate with the $I^-(^1S_0) + I^+(^3P_2)$ reactants state are displayed here.

determinants spanned by the p^5 manifold of each of the iodine atoms (thus representing 10 electrons in 12 spinors). For further information, readers can consult the computational details section of Poline *et al.* [9].

It should be noted that we computed the potential energy curves for states with projection of total electronic angular momentum $\Omega = 0, 1, 2$ but not for states with $\Omega > 2$ since the $I^-(^1S_0) + I^+(^3P_2)$ reactant state does not correlate with such states. Indeed, the $I^-(^1S_0) + I^+(^3P_2)$ state correlates with states having the following angular momenta [14]: the double degenerate $(\Omega = 1)_g$, $(\Omega = 1)_u$, $(\Omega = 2)_g$, and $(\Omega = 2)_u$, and the singly degenerate $(\Omega = 0)_g^+$ and $(\Omega = 0)_u^+$.

Furthermore, for implementation reasons the KRICI module does not take into account the +/- symmetry and thus is not able to differentiate directly the + and the - states. In order to do that, we also computed the dipole transition moments between the $(\Omega = 0)_g$ and the $(\Omega = 0)_u$ states. Knowing that the lowest $(\Omega = 0)_g$ state is of + symmetry and that the lowest $(\Omega = 0)_u$ state is of - symmetry [14], we were able to rebuild the potential energy curves of the $(\Omega = 0)_g^+$ and $(\Omega = 0)_u^+$ states using the selection rule stating that the dipole transition between a + and a - state is forbidden [15]. The list of the computed states and their asymptotic energies are reported in Table I.

B. Landau-Zener surface hopping

An accurate description of MN reactions at low collision energies requires, in principle, a fully quantum mechanical approach for the nuclear dynamics. However, in the current system, such a sophisticated approach is out of reach from a computational point of view: nonadiabatic couplings are not implemented in the KRICI module of the DIRAC package. Moreover, the potential energy curves of I_2 exhibit multiple and overlapping avoided crossings such that a diabaticization

procedure would be a tedious and challenging task. To overcome this difficulty, in this work we employ the LZSH method [17] to obtain the cross sections of the $I^+ + I^-$ mutual neutralization reaction.

LZSH is a probabilistic, semiclassical method in which the system is moving classically along the potential energy curves. The nonadiabatic interactions are considered only at the vicinity of avoided crossings [18,19]. The list of the avoided crossings considered in this work is given in Table IV of the Appendix. Note that, as previously mentioned in Poline *et al.* [9], we estimated the electronic couplings at large-distance ($R > 7 \text{ \AA}$) crossings between the ion-pair states and the $I(5p^46s) + I(^2P_{1/2})$ states. These couplings have been shown to be negligible (see below).

The LZSH method can be described as follows: The system starts at a distance R_0 on the curve corresponding to the reactants [i.e., the curves which correlate with the $I^-(^1S_0) + I^+(^3P_2)$ ion pair state], R_0 being larger than the internuclear distances of all avoided crossings [in this work, $R_0 = 12$ atomic units (a.u.)]. The system then moves along this curve while it has sufficient kinetic energy and until it reaches an avoided crossing. At this point there is a probability $p_{\alpha \rightarrow \beta}^{LZ}$ [given by the Landau-Zener formula [20–22], Eq. (1)] that the system hops from its starting state (named α) to the other state involved in the avoided crossing (named β), if its kinetic energy is sufficient. We have

$$p_{\alpha \rightarrow \beta}^{LZ} = \exp\left(-\frac{\pi}{2v} \sqrt{\frac{\Delta V_{\alpha\beta}^3}{\frac{d^2}{dR^2}(\Delta V_{\alpha\beta})}}\right), \quad (1)$$

where v is the relative radial velocity of the two nuclei at the crossing and $\Delta V_{\alpha\beta}$ is the energy difference between the two adiabatic potential energy curves at the avoided crossing. v is

TABLE I. Asymptotic energies of the I₂ states employed in this work. The molecular states are identified by the projection of the total electronic angular momentum (Ω). The number of states for each Ω symmetry are given in parentheses. The last four states of this table correspond to ion-pair states.

| Dissociation limits | Molecular states | Asymptotic energy (eV) | |
|---|---|------------------------|----------|
| | | MRCI (this work) | Exp [16] |
| ² P _{3/2} + ² P _{3/2} | 2 _g (1), 1 _g (1), 0 _g ⁺ (2), 2 _u (1), 1 _u (2), 0 _u ⁻ (2) | 0 | 0 |
| ² P _{1/2} + ² P _{3/2} | 2 _g (1), 1 _g (2), 0 _g ⁺ (1), 0 _g ⁻ (1), 2 _u (1), 1 _u (2), 0 _u ⁺ (1), 0 _u ⁻ (1), | 1.04 | 0.943 |
| ² P _{1/2} + ² P _{1/2} | 0 _g ⁺ (1), 1 _u (1), 0 _u ⁻ (1) | 1.99 | 1.885 |
| ² [2] _{5/2} + ² P _{3/2} | 2 _g (3), 1 _g (4), 0 _g ⁺ (2), 0 _g ⁻ (2), 2 _u (3), 1 _u (4), 0 _u ⁺ (2), 0 _u ⁻ (2) | 7.23 | 6.774 |
| ² [2] _{3/2} + ² P _{3/2} | 2 _g (2), 1 _g (3), 0 _g ⁺ (2), 0 _g ⁻ (2), 2 _u (2), 1 _u (3), 0 _u ⁺ (2), 0 _u ⁻ (2) | 7.41 | 6.954 |
| ¹ S ₀ + ³ P ₂ | 2 _g (1), 1 _g (1), 0 _g ⁺ (1), 2 _u (1), 1 _u (1), 0 _u ⁺ (1) | 7.24 | 7.392 |
| ¹ S ₀ + ³ P ₁ | 1 _g (1), 0 _g ⁻ (1), 1 _u (1), 0 _u ⁻ (1) | 8.13 | 8.191 |
| ¹ S ₀ + ³ P ₀ | 0 _g ⁺ (1), 0 _u ⁺ (1) | 8.22 | 8.271 |
| ¹ S ₀ + ¹ D ₂ | 2 _g (1), 1 _g (1), 0 _g ⁺ (1), 2 _u (1), 1 _u (1), 0 _u ⁺ (1) | 9.00 | 9.094 |

simply obtained by energy conservation,

$$v = \sqrt{\frac{2[E_m - V_{\text{eff},\alpha}(R)]}{\mu}}, \quad (2)$$

with μ being the reduced mass of the system (for I₂, $\mu = 115666$ a.u.). $V_{\text{eff},\alpha}(R)$ is the effective adiabatic potential energy of the state α at the internuclear distance R ,

$$V_{\text{eff},\alpha}(l, R) = V_{\alpha}(R) + \frac{l(l+1)}{2\mu R^2}. \quad (3)$$

E_m is the mechanical energy of the system,

$$E_m = E_{\text{coll}} + V_{\text{asyp}} \quad (4)$$

where E_{coll} is the collision energy in the center of mass frame and V_{asyp} is the energy of the I⁻(¹S₀) + I⁺(³P₂) reactant state at $R \rightarrow +\infty$.

When the kinetic energy of the system reaches 0, the system turns back, and when it reaches R_0 again, the trajectory ends. By computing a sufficiently high number of trajectories, we can compute a reaction probability P_f towards each of the possible product states f :

$$P_f = \frac{N_f}{N_{\text{tot}}}, \quad (5)$$

where N_f is the number of trajectories which ended in the product state f and N_{tot} is the total number of trajectories. In this work we used $N_{\text{tot}} = 400$. We found that using a higher value of N_{tot} has no significant impact on the results.

The cross sections towards each product state are then obtained by integrating the P_f over the angular momentum l [23],

$$\sigma_f^X(E_{\text{coll}}) = \frac{\pi}{2\mu E_{\text{coll}}} \sum_{l=0}^{l=+\infty} (2l+1)P_f(E_{\text{coll}}, l), \quad (6)$$

where X denotes a given symmetry state of the I₂ potential energy curves.

Practically, the sum in Eq. (6) stops (at a value $l = l_{\text{max}}$) when the rotational barrier becomes too important for the system to reach the farthest avoided crossing involving the

reactant state. We have

$$l_{\text{max}} = -\frac{1}{2} + \sqrt{\frac{1}{4} - \frac{\mu R_c^2}{2}(4V(R_c) - V_{\text{asyp}} - E_{\text{coll}})}, \quad (7)$$

where R_c and $V(R_c)$ are the internuclear distance and the adiabatic energy of the reactant state at this avoided crossing.

This approach is used for each of the symmetries considered in this work (see Sec. II A), and the reaction cross sections towards each state are then obtained by averaging over all symmetries, taking into account their multiplicity, hence

$$\sigma_f(E_{\text{coll}}) = \frac{\sum_{X \in \text{symmetries}} m_X \sigma_f^X(E_{\text{coll}})}{\sum_{X \in \text{symmetries}} m_X}, \quad (8)$$

with m_X being the multiplicity of the symmetry X and σ_f^X the reaction cross section towards the state α for the symmetry X obtained with Eq. (6).

At large distance ($R > 7 \text{ \AA}$), the avoided crossings between the ion-pair states and the I(5p⁴6s) + I(²P_{1/2}) states are not described by the MRCI calculations presented in Sec. II A. For the avoided crossings between the ion pair states I⁻(¹S₀) + I⁺(³P₂), I⁻(¹S₀) + I⁺(³P₁) and the I(5p⁴6s) + I(²P_{1/2}) states we used a semiempirical model to estimate the electronic couplings (see Olson *et al.* [24], Eq. (13), using $\frac{\gamma^2}{2} = 3.059 \text{ eV}$ [25]). We obtained coupling values that are less than $8 \cdot 10^{-5}$ a.u.. These avoided crossings take place at sufficiently large distances for the semiempirical model to be valid. However, the avoided crossings between the ion pair states I⁻(¹S₀) + I⁺(¹D₂) and the I(5p⁴6s) + I(²P_{1/2}) states take place at shorter distances and thus were described by computing the potential energy curves of the system (using the same method as the one described in Sec. II A), with 21 points with an internuclear distance varying from 7 to 8 \AA . We obtained coupling values that are less than 6×10^{-5} a.u.. Including these avoided crossings in our calculation was shown to have no significant effect on the results (less than 0.2% difference on the cross sections).

C. Empirical correction to the asymptotic energies

When comparing the asymptotic energies obtained with the MRCI method and the experimental values (see Table I), we noticed that the MRCI asymptotic energies of the neutral

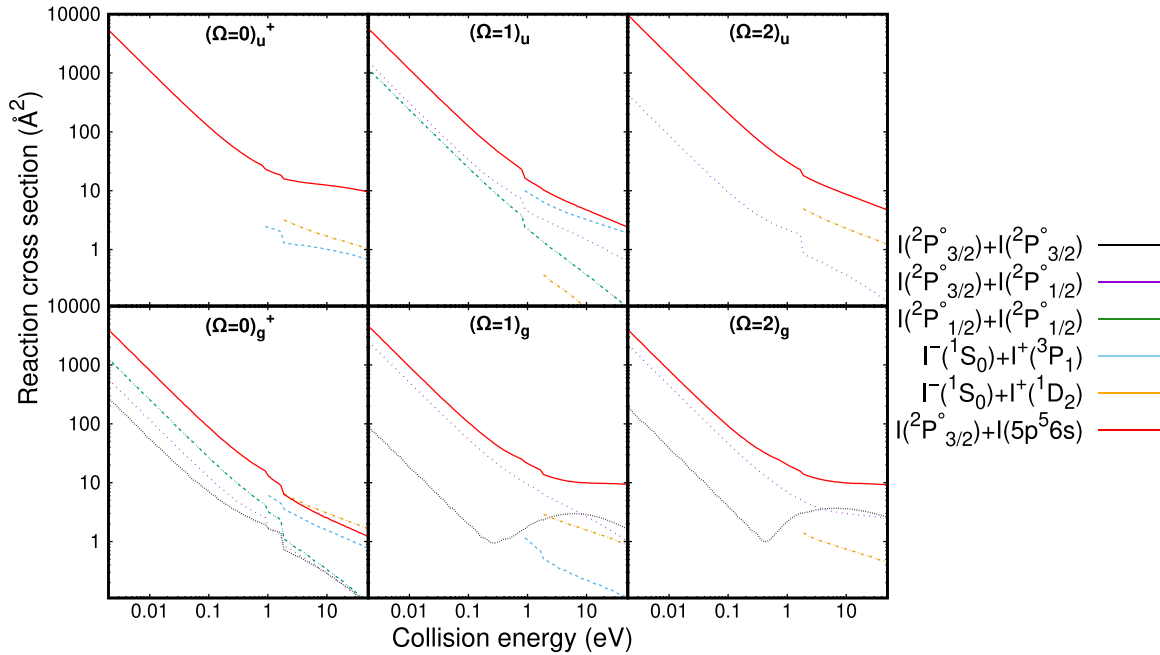


FIG. 2. Cross sections for the reactions between I^+ and I^- for the six symmetries correlating with the $I^-(^1S_0) + I^+(^3P_2)$ reactants state.

states are overestimated while the MRCI asymptotic energy of the ion pair states is underestimated. For the three lowest neutral product states and the excited ion pair products, the difference between the asymptotic energies of the reactant and product states are satisfactory within the MRCI method (between 3% and 12% of error). However, the differences of asymptotic energy between the reactant and the $5p^46s$ states [$I(^2[2]_{3/2}) + I(^2P_{5/2})$ and $I(^2[2]_{3/2}) + I(^2P_{3/2})$ states] are not well reproduced. The path towards the $I(^2[2]_{3/2}) + I(^2P_{5/2})$ state is open only by 0.01 eV in the MRCI calculation while it should be open with an asymptotic energy difference of 0.62 eV, and the path towards the $I(^2[2]_{3/2}) + I(^2P_{3/2})$ state is closed while it should be open with an asymptotic energy difference of 0.44 eV. To correct for this qualitative and quantitative failure, we decided to increase artificially the asymptotic energy of the ion pair states by a quantity ϵ in order to reproduce the experimental asymptotic energy difference between the $I(^2[2]_{3/2}) + I(^2P_{5/2})$ and the $I^-(^1S_0) + I^+(^3P_2)$. The value of ϵ is 0.61 eV. This is the only departure from the underlying *ab initio* energy curves in our work.

III. RESULTS AND DISCUSSION

Using the potential energy curves presented in Sec. II A, we applied the LZSH method for each of the symmetries considered here (see Sec. II A). We thus obtained the reaction cross sections towards the following neutral product states: $I(^2P_{3/2}) + I(^2P_{3/2})$, $I(^2P_{3/2}) + I(^2P_{1/2})$, $I(^2P_{1/2}) + I(^2P_{1/2})$, and $I(5p^46s) + I(^2P_{1/2})$.

Here, we did not try to differentiate the different substates constituting the $I(5p^46s)$ configuration obtained with the MRCI method, since the energy difference between some of these substates is below 0.2 eV [16]. We lack extensive benchmark studies between MRCI and other approaches such as those based on coupled cluster wave functions for the iodine systems. However, from recent examples in the literature

[26–28] in which a comparison of methods has been made on an equal footing (same basis set and Hamiltonian), we see that among different correlated approaches, the corresponding electronic state energies can differ by values which are similar to, or higher than, the differences among substates seen here.

We also obtained the reaction cross sections towards the two lowest-energy excited ion-pair states $I^-(^1S_0) + I^+(^3P_1)$ and $I^-(^1S_0) + I^+(^1D_2)$. The evolution of these reaction cross sections with respect to the collision energy is shown in Fig. 2 and the total symmetrized reaction cross sections, obtained with Eq. (8), are shown in Fig. 3.

At collision energies lower than 0.1 eV the cross sections towards the neutral product states follow an asymptotic behavior proportional to the inverse of the collision energy. At these energies, for all symmetries, the most abundant product is the neutral $I(5p^46s) + I(^2P_{1/2})$ product, followed by

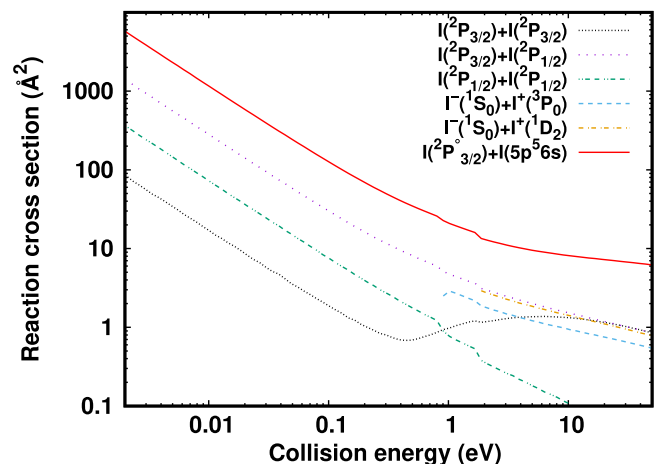


FIG. 3. Total (symmetry averaged) cross sections for the $I^+ + I^- \rightarrow 2I$ and $I^+ + I^- \rightarrow (I^+)^* + I^-$ reactions.

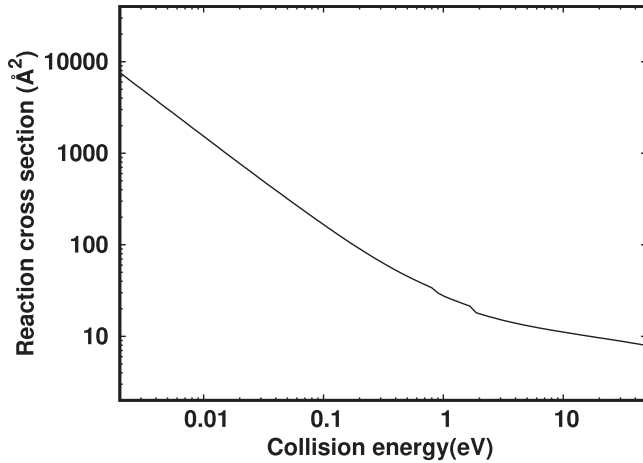


FIG. 4. Total (symmetry averaged) cross section for mutual neutralization cross section between I^+ and I^- .

the three lowest-energy neutral products $I(^2P_{3/2}) + I(^2P_{3/2})$, $I(^2P_{3/2}) + I(^2P_{1/2})$, and $I(^2P_{1/2}) + I(^2P_{1/2})$, in this order.

At collision energies higher than 0.3 eV the cross sections towards the $I(^2P_{3/2}) + I(^2P_{3/2})$ state increase up to the collision energy of 10 eV, while the cross sections towards the

$I(^2P_{1/2}) + I(^2P_{3/2})$ and $I(5p^46s) + I(^2P_{1/2})$ states decrease at a slower rate than for the collision energies below 0.1 eV. At collision energies higher than 0.1 eV the cross sections towards the $I(^2P_{1/2}) + I(^2P_{1/2})$ state continue to decrease as the inverse of the collision energy, so it becomes negligible compared to the other cross sections.

The reaction cross sections towards the $I^-(^1S_0) + I^+(^3P_1)$ and $I^-(^1S_0) + I^+(^1D_2)$ ion pair states have energy thresholds of, respectively, 0.26 eV and 1.1 eV. The values of these cross sections after their threshold are of the same order of magnitude as the one of the $I(^2P_{1/2}) + I(^2P_{3/2})$ state.

The total of the neutralization cross sections (sum of the cross sections toward all neutral states) is shown in Fig. 4. It decreases as the inverse of the collision energy up to 0.1 eV and then decreases at a slower rate. The two discontinuities at 0.26 eV and 1.1 eV correspond to the energy thresholds of the reactions producing the two excited ion pairs.

In 2021, Poline *et al.* [9] conducted an experiment at the double ion storage ring DESIREE in Stockholm. They were able to measure the branching ratios towards each of the neutral product states—more specifically, they obtained the ratio (denoted by R_σ) between the $I(5p^46s) + I(^2P_{1/2})$ states and the $I(^2P_{3/2}) + I(^2P_{3/2})$, $I(^2P_{3/2}) + I(^2P_{1/2})$, and $I(^2P_{1/2}) + I(^2P_{1/2})$ states, for collision energy of 0.1 and 0.8 eV. We therefore have R_σ as

$$R_\sigma = \frac{\sigma[I(^2P_{3/2}) + I(^2P_{3/2})] + \sigma[I(^2P_{3/2}) + I(^2P_{1/2})] + \sigma[I(^2P_{1/2}) + I(^2P_{1/2})]}{\sigma[I(5p^46s) + I(^2P_{1/2})] + \sigma[I(^2P_{3/2}) + I(^2P_{3/2})] + \sigma[I(^2P_{3/2}) + I(^2P_{1/2})] + \sigma[I(^2P_{1/2}) + I(^2P_{1/2})]} \quad (9)$$

We can directly obtain this ratio from our calculations. The comparison between the theoretical ratio and the measurements is shown in Fig. 5. Our results show that this branching ratio does not vary significantly with respect to the collision energy, with values between 22% and 27%. The measured and computed ratio are of the same order of magnitude. However, the LZSH-based model underestimates this ratio by a factor of 1.5.

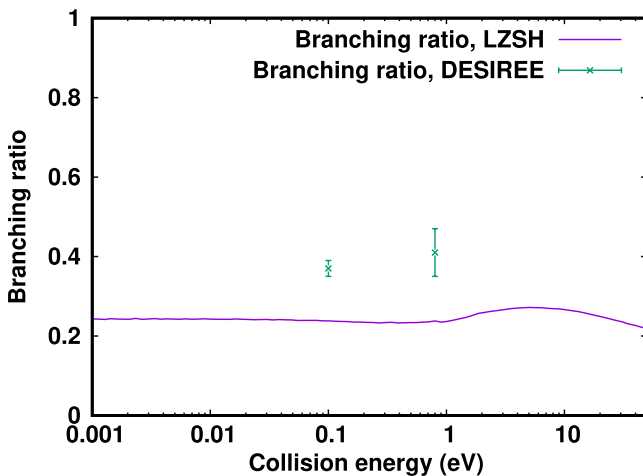


FIG. 5. Comparison of the R_σ ratios, computed with the LZSH method and measured by Poline *et al.* [9].

Moreover, our model gives a semiquantitative agreement for the prediction of the ratios between the cross sections of the $I(^2P_{3/2}) + I(^2P_{3/2})$, $I(^2P_{3/2}) + I(^2P_{1/2})$, and $I(^2P_{1/2}) + I(^2P_{1/2})$ states. These ratios, in comparison with those obtained by Poline *et al.* [9], are displayed in Table II.

Poline *et al.* [9] were also able to estimate the absolute neutralization cross section, at a collision energy of 0.1 eV, to be in the range of $10^{3 \pm 1} \text{ \AA}^2$. Our results displayed in Fig. 4 (165 \AA^2 at 0.1 eV) agree with this estimation.

The disagreement between the experiments at DESIREE and our results may be attributed to the semiclassical approach employed in this work. However, given the complexity of the studied collisional system and the lack of data on the considered MN reaction, such semiquantitative estimates represent a significant step toward a better modeling, and thus understanding, of iodine plasma.

TABLE II. Ratios of the cross sections between the three lowest neutral product states, obtained with the LZSH method and experimentally by Poline *et al.* [9] at collision energy of 0.1 and 0.8 eV.

| Product channel | 0.1 eV | | 0.8 eV | |
|-------------------------------|--------|------|--------|------|
| | LZSH | exp. | LZSH | exp. |
| $I(^2P_{3/2}) + I(^2P_{3/2})$ | 5% | 31% | 12% | 28% |
| $I(^2P_{3/2}) + I(^2P_{1/2})$ | 76% | 57% | 76% | 51% |
| $I(^2P_{1/2}) + I(^2P_{1/2})$ | 19% | 11% | 13% | 21% |

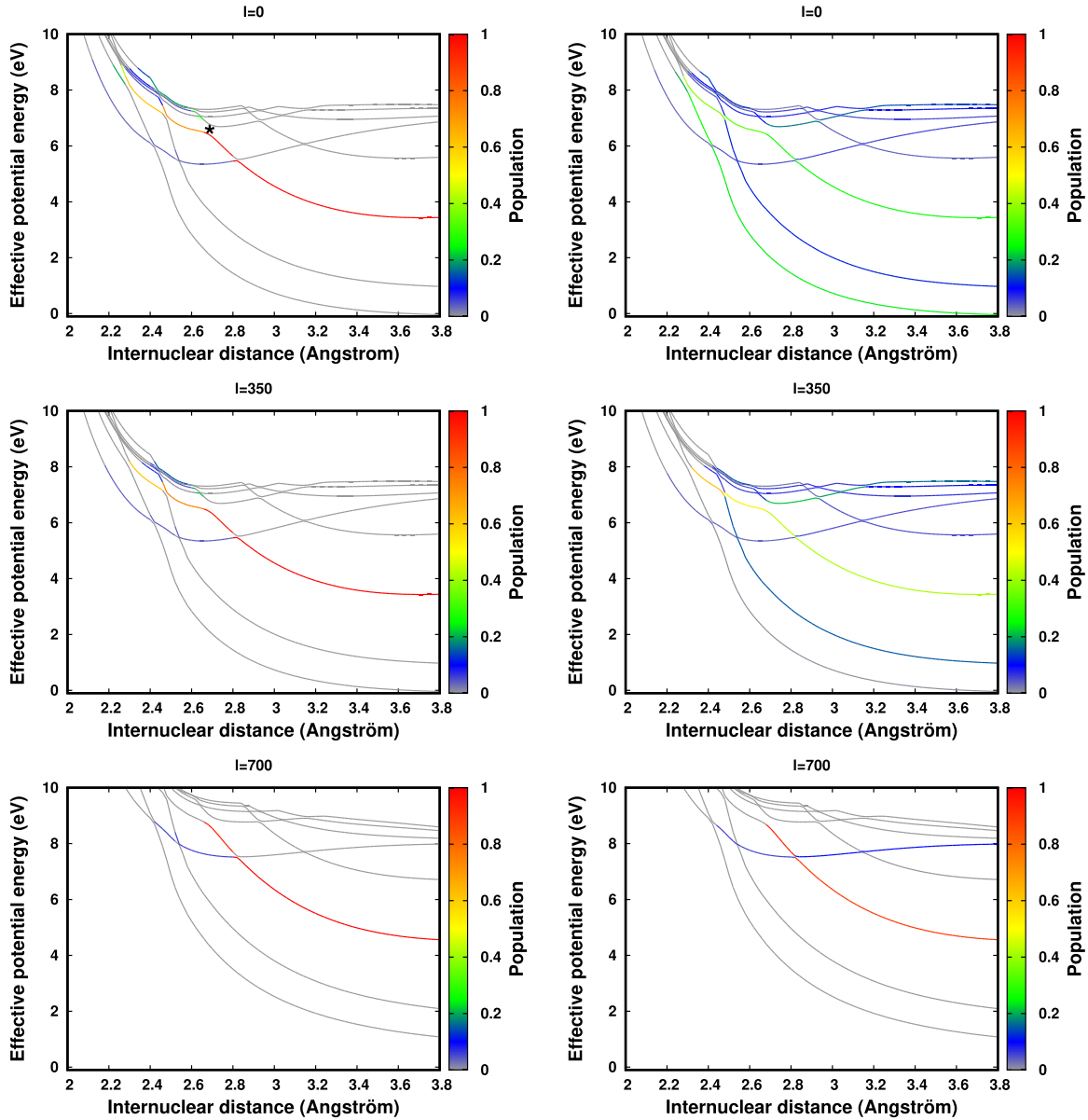


FIG. 6. Effective potential energy curves of the first eight states of the $(\Omega = 2)_g$ symmetry for three different values of angular momentum. The population $n_\alpha^-(R)$ [$n_\alpha^+(R)$] is displayed with a color scheme in the left (right) panel. At $t = 0$, the population is 1 in the lowest ion-pair state (the third state in energy order) and 0 in all the other states

In order to gain more insight into the dynamics of the MN reaction, we investigate which avoided crossings contribute the most to the reactivity. We computed statistically the population on each state as a function of time [$n_\alpha(t)$],

$$n_\alpha(t) = \frac{N_\alpha(t)}{N_{\text{traj}}}, \quad (10)$$

where $N_\alpha(t)$ is the number of trajectories on the state α at the time t . Since the time does not appear explicitly in the method described in Sec. II B, we computed it *a posteriori* by integrating Newton's law of motion [see Eq. (11), with r_i , r_j being two adjacent points of the potential energy surface and v being the speed of the system]. The time is set arbitrarily at 0 when a trajectory starts at R_0 . N_{traj} is the total number of

computed trajectories.

$$\begin{aligned} \Delta t_{ji} &= \frac{\sqrt{2\mu}}{B} (\sqrt{E_m - V(r_j)} - \sqrt{E_m - V(r_i)}) \text{ if } R \text{ decreases} \\ \Delta t_{ij} &= \frac{\sqrt{2\mu}}{B} (\sqrt{E_m - V(r_i)} - \sqrt{E_m - V(r_j)}) \text{ if } R \text{ increases,} \end{aligned} \quad (11)$$

with $\Delta t_{lk} = t(r_l) - t(r_k)$ and $B = [V(r_j) - V(r_i)]/(r_j - r_i)$.

For each of the symmetries considered in this work we computed $N_{\text{traj}} = 10\,000$ trajectories, for a collision energy of 0.9 eV and three different values of the angular momentum l ($l = 0$, $l = 350$, and $l = 700$). The populations obtained with these trajectories are then computed using Eq. (10) for each of the electronic states considered in this work. The population on each of the first eight electronic states of the $(\Omega = 2)_g$ symmetry are displayed in Fig. 6. For clarity we choose to

TABLE III. Diffuse exponents used in the electronic structure calculations for the iodine atom. These were added to the dyall.v3z basis set.

| Primitive type | Exponents |
|----------------|-----------|
| s | 0.0395300 |
| | 0.0175618 |
| | 0.0078021 |
| p | 0.0285513 |
| | 0.0112589 |
| | 0.0044398 |
| d | 0.0773620 |
| | 0.0321000 |
| | 0.0133193 |
| f | 0.1159934 |
| | 0.0331410 |
| | 0.0094689 |

represent separately the population $n_{\alpha}^{\leftarrow}(R)$ coming from the part of the trajectories with decreasing values of R (before reaching the closest approach distance) and the population $n_{\alpha}^{\rightarrow}(R)$ coming from the part of the trajectories with increasing values of R (after reaching the closest approach distance), which are given by

$$n_{\alpha}^{\leftarrow}(R) = \frac{N_{\alpha}^{\leftarrow}(R)}{N_{\text{tot}}} \quad \text{and} \quad n_{\alpha}^{\rightarrow}(R) = \frac{N_{\alpha}^{\rightarrow}(R)}{N_{\text{tot}}}, \quad (12)$$

with $N_{\alpha}^{\leftarrow}(R)$ [$N_{\alpha}^{\rightarrow}(R)$] being the number of trajectories crossing the internuclear distance R before (after) reaching the closest approach distance. In Fig. 6, $n_{\alpha}^{\leftarrow}(R)$ [$n_{\alpha}^{\rightarrow}(R)$] is shown in the left (right) panel of the figure using a color scheme traced on the effective potential energy curves [see Eq. (3)] of the $(\Omega = 2)_g$ symmetry.

At the first avoided crossing reached by the system (at 2.8 Å), it mainly has a diabatic behavior with approximately 90% of the population transferred to the higher energy state. This behavior is observed for the majority of the avoided crossings of the system, with the important exception of the crossing between the fourth and fifth states (in increasing energy order) at 2.7 Å (marked with a star in Fig. 6). For this crossing we mainly observe an adiabatic behavior, but still with an important percentage of the population (about 30%) transferred to the higher energy state. This intermediate behavior is directly responsible for the reactivity towards the I* states, and indirectly responsible for the reactivity towards the lowest energy states through the avoided crossings between the third and fourth states at 2.5 Å and between the second and third states at 2.3 Å. The path towards the lowest energy states is the first to be screened by the rotational barrier. A chemical reaction towards those states is thus only possible for collisions with a low impact parameter (the link between the impact parameter b and the angular momentum l is given by $l = \sqrt{2\mu E_{\text{coll}}} \times b$ [23]).

The reactions towards the I($5p^46s$) + I($^2P_{3/2}$) states are still possible at higher values of l , which explains the higher reactivity towards those states (see Fig. 5). The populations were also computed for the other symmetries. We did not find any major difference in the behavior of the

TABLE IV. List of the avoided crossings considered in this work. For each avoided crossing we give its internuclear distance and the index of the two electronic states concerned by this crossing. The electronic states indexes are given by their energetic order (starting from zero for the lowest energy state of each symmetry)

| Symmetry | Lower state | Higher state | R (Å) |
|--------------------|-------------|--------------|---------|
| $(\Omega = 0)_g^+$ | 3 | 4 | 2,30 |
| | 2 | 3 | 2,36 |
| | 5 | 6 | 2,36 |
| | 4 | 5 | 2,39 |
| | 1 | 2 | 2,42 |
| | 3 | 4 | 2,42 |
| | 2 | 3 | 2,46 |
| | 5 | 6 | 2,48 |
| | 4 | 5 | 2,51 |
| | 3 | 4 | 2,54 |
| | 2 | 3 | 2,66 |
| | 5 | 6 | 2,74 |
| | 6 | 7 | 2,78 |
| | 4 | 5 | 2,82 |
| | 5 | 6 | 2,86 |
| 7 | 8 | 2,96 | |
| 7 | 8 | 3,15 | |
| 6 | 7 | 3,18 | |
| 7 | 8 | 3,28 | |
| $(\Omega = 0)_u^+$ | 4 | 5 | 2,42 |
| | 3 | 4 | 2,48 |
| | 1 | 2 | 2,48 |
| | 2 | 3 | 2,54 |
| | 1 | 2 | 2,58 |
| | 4 | 5 | 2,62 |
| | 3 | 4 | 2,64 |
| | 2 | 3 | 2,68 |
| | 4 | 5 | 2,76 |
| | 3 | 4 | 2,86 |
| | 4 | 5 | 2,90 |
| 3 | 4 | 2,92 | |
| $(\Omega = 1)_g$ | 5 | 6 | 2,24 |
| | 4 | 5 | 2,26 |
| | 6 | 7 | 2,29 |
| | 3 | 4 | 2,31 |
| | 2 | 3 | 2,33 |
| | 5 | 6 | 2,34 |
| | 1 | 2 | 2,35 |
| | 4 | 5 | 2,37 |
| | 3 | 4 | 2,38 |
| | 0 | 1 | 2,42 |
| | 6 | 7 | 2,42 |
| | 5 | 6 | 2,44 |
| | 2 | 3 | 2,44 |
| | 4 | 5 | 2,46 |
| | 1 | 2 | 2,48 |
| 3 | 4 | 2,48 | |
| 2 | 3 | 2,53 | |
| 7 | 8 | 2,67 | |
| 6 | 7 | 2,70 | |
| 5 | 6 | 2,71 | |
| 4 | 5 | 2,76 | |
| 8 | 9 | 2,77 | |
| 7 | 8 | 2,78 | |

TABLE IV. (*Continued*)

| Symmetry | Lower state | Higher state | R (Å) |
|------------------|-------------|--------------|---------|
| | 6 | 7 | 2,80 |
| | 3 | 4 | 2,84 |
| | 8 | 9 | 2,85 |
| | 5 | 6 | 2,86 |
| | 7 | 8 | 2,87 |
| | 4 | 5 | 2,94 |
| | 6 | 7 | 2,96 |
| | 8 | 9 | 2,99 |
| | 5 | 6 | 3,06 |
| | 7 | 8 | 3,25 |
| $(\Omega = 1)_u$ | 6 | 7 | 2,34 |
| | 5 | 6 | 2,36 |
| | 3 | 5 | 2,42 |
| | 2 | 3 | 2,46 |
| | 6 | 8 | 2,46 |
| | 6 | 7 | 2,50 |
| | 5 | 6 | 2,52 |
| | 4 | 5 | 2,54 |
| | 7 | 9 | 2,54 |
| | 6 | 7 | 2,56 |
| | 3 | 4 | 2,56 |
| | 5 | 6 | 2,58 |
| | 4 | 5 | 2,60 |
| | 9 | 10 | 2,64 |
| | 7 | 8 | 2,64 |
| | 6 | 7 | 2,70 |
| | 8 | 9 | 2,70 |
| | 7 | 8 | 2,86 |
| | 8 | 9 | 2,90 |
| | 6 | 8 | 2,92 |
| | 9 | 10 | 3,06 |
| | 8 | 9 | 3,10 |
| | 7 | 8 | 3,14 |
| $(\Omega = 2)_g$ | 2 | 6 | 2,24 |
| | 3 | 4 | 2,24 |
| | 1 | 2 | 2,30 |
| | 6 | 7 | 2,42 |
| | 0 | 1 | 2,42 |
| | 4 | 6 | 2,44 |
| | 3 | 4 | 2,46 |
| | 1 | 2 | 2,54 |
| | 6 | 7 | 2,61 |
| | 2 | 3 | 2,49 |
| | 5 | 6 | 2,62 |
| | 4 | 5 | 2,64 |
| | 3 | 4 | 2,68 |
| | 2 | 3 | 2,82 |
| | 6 | 7 | 2,86 |
| | 5 | 6 | 2,88 |
| | 4 | 5 | 2,94 |
| | 6 | 7 | 2,94 |
| | 5 | 6 | 3,04 |
| | 3 | 4 | 3,14 |
| | 6 | 7 | 3,16 |
| $(\Omega = 2)_u$ | 3 | 4 | 2,48 |
| | 6 | 7 | 2,50 |
| | 5 | 6 | 2,50 |

TABLE IV. (*Continued*)

| Symmetry | Lower state | Higher state | R (Å) |
|----------|-------------|--------------|---------|
| | 4 | 5 | 2,51 |
| | 3 | 4 | 2,52 |
| | 2 | 3 | 2,55 |
| | 1 | 2 | 2,56 |
| | 4 | 5 | 2,64 |
| | 6 | 7 | 2,70 |
| | 5 | 7 | 2,74 |
| | 4 | 5 | 2,78 |
| | 3 | 4 | 2,82 |
| | 2 | 3 | 2,84 |
| | 6 | 7 | 2,86 |
| | 4 | 5 | 2,90 |
| | 5 | 6 | 2,92 |
| | 4 | 5 | 2,94 |
| | 3 | 4 | 2,98 |
| | 6 | 7 | 3,15 |

populations between the $(\Omega = 2)_g$ symmetry and the other symmetries.

IV. CONCLUSION

As a first step towards the generation of accurate models for the reactivity in iodine plasmas, in this work we have investigated a computational protocol, combining four-component multireference CI calculations for the I_2 system to obtain potential energy curves and the semiclassical Landau-Zener surface hopping method to treat nuclear dynamics, to obtain theoretical cross sections of the mutual neutralization reaction between I^+ and I^- for collision energies varying from 0.001 eV to 50 eV.

Our results agree qualitatively with the recent experimental measurements performed at the double ion ring DESIREE facility in the overlapping collision energy range. Furthermore, our work provides absolute cross sections over a broad range of collision energy. Our results show that the total cross section decrease from 1000 \AA^2 at 0.001 eV collision energy to about 10 \AA^2 at 10 eV impact energy. Moreover, the branching ratios towards the different final states do not vary significantly with respect to the collision energy. We also studied the dynamics of this mutual neutralization reaction.

The data and insights provided in this work will allow to model, beyond the current state of the art, the chemistry taking place in iodine plasma, which is particularly relevant for electric space propulsion.

ACKNOWLEDGMENTS

S.B. thanks the École normale supérieure Paris-Saclay for the PhD scholarship. X.Y. and A.S.P.G. acknowledge funding from projects ComprIXS (No. ANR-19-CE29-0019 and No. DFG JA 2329/6-1), Labex CaPPA (No. ANR-11-LABX-0005-01), and the I-SITE ULNE project OVERSEE and MESONM International Associated Laboratory (LAI) (No. ANR-16-IDEX-0004), and support from the French national supercomputing facilities (Grants No. DARI A0090801859 and No. A0110801859). P.L.B. and N.S. thank Institut

Physique des Infinis for financial support. S.B., P.L.B., and N.S. thank the members of the DESIREE facility for their warm welcome. The authors would also like to thank A. Bourdon, J.-P. Booth, and B. Esteves for their interest in our work.

APPENDIX

The diffuse functions used to describe accurately Rydberg and ion-pair states are given in Table III. Table IV reports the list of the avoided crossings considered in this work.

-
- [1] N. S. Shuman, D. E. Hunton, and A. A. Viggiano, *Chem. Rev.* **115**, 4542 (2015).
- [2] A. B. Fialkov, *Prog. Energy Combust. Sci.* **23**, 399 (1997).
- [3] D. Smith, N. G. Adams, and M. J. Church, *Planet. Space Sci.* **24**, 697 (1976).
- [4] D. Smith, *Chem. Rev.* **92**, 1473 (1992).
- [5] W. L. Morgan, J. N. Bardsley, J. Lin, and B. L. Whitten, *Phys. Rev. A* **26**, 1696 (1982).
- [6] Å. Larson, J. Hörnquist, P. Hedvall, and A. E. Orel, *J. Chem. Phys.* **151**, 214305 (2019).
- [7] D. Rafalskyi, J. M. Martínez, L. Habl, E. Zorzoli Rossi, P. Proynov, A. Boré, T. Baret, A. Poyet, T. Laffleur, S. Dudin, and A. Aanesland, *Nature (London)* **599**, 411 (2021).
- [8] B. Esteves, F. Marmuse, C. Drag, A. Bourdon, A. Alvarez Laguna, and P. Chabert, *Plasma Sources Sci. Technol.* **31**, 085007 (2022).
- [9] M. Poline, X. Yuan, S. Badin, M. C. Ji, S. Rosén, S. Indrajith, R. D. Thomas, H. T. Schmidt, H. Zettergren, A. S. P. Gomes, and N. Sisourat, *Phys. Rev. A* **106**, 012812 (2022).
- [10] T. Fleig, J. Olsen, and L. Visscher, *J. Chem. Phys.* **119**, 2963 (2003).
- [11] T. Saue, R. Bast, A. S. P. Gomes, H. J. A. Jensen, L. Visscher, I. A. Aucar, R. D. Remigio, K. G. Dyall, E. Eliav, E. Fasshauer, T. Fleig, L. Halbert, E. D. Hedegård, B. Helmich-Paris, M. Iliaš, C. R. Jacob, S. Knecht, J. K. Laerdahl, M. L. Vidal, M. K. Nayak *et al.*, *J. Chem. Phys.* **152**, 204104 (2020).
- [12] A. S. P. Gomes, T. Saue, L. Visscher, H. J. A. Jensen, R. Bast, I. A. Aucar, V. Bakken, K. G. Dyall, S. Dubillard, U. Ekström, E. Eliav, T. Enevoldsen, E. Fasshauer, T. Fleig, O. Fossgaard, L. Halbert, E. D. Hedegård, T. Helgaker, B. Helmich-Paris, J. Henriksson *et al.*, “DIRAC19” (2019).
- [13] K. G. Dyall, *Theor. Chem. Acc.* **115**, 441 (2006).
- [14] S. Lukashov, A. Petrov, and A. Privilov, The iodine molecule: Insights into intra- and intermolecular perturbation in diatomic molecules (2018).
- [15] C. N. Banwell, *Fundamentals of Molecular Spectroscopy*, 3rd ed. (McGraw-Hill, London, 1983).
- [16] A. Kramida, Yu. Ralchenko, J. Reader, and NIST ASD Team, (2019), NIST Atomic Spectra Database (ver. 5.7.1), [Online]. Available: <https://physics.nist.gov/asd> [2020, September 30]. National Institute of Standards and Technology, Gaithersburg, MD.
- [17] A. K. Belyaev, C. Lasser, and G. Trigila, *J. Chem. Phys.* **140**, 224108 (2014).
- [18] M. Desouter-Lecomte, Y. Justum, and X. Chapuisat, in *Introduction la Théorie Quantique: Concepts, Pratiques et Applications* (2017).
- [19] E. Wigner and E. E. Witmer, in *World Scientific Series in 20th Century Chemistry* (World Scientific, Singapore, 2000), Vol. 8, pp. 287–311.
- [20] C. Zener, *Proc. R. Soc. London, Ser. A* **137**, 696 (1932).
- [21] A. K. Belyaev and O. V. Lebedev, *Phys. Rev. A* **84**, 014701 (2011).
- [22] O. V. Ivakhnenko, S. N. Shevchenko, and F. Nori, *Phys. Rep.* **995**, 1 (2023).
- [23] M. S. Child, *Molecular Collision Theory* (Academic, London, 1974).
- [24] R. E. Olson, J. R. Peterson, and J. Moseley, *J. Chem. Phys.* **53**, 3391 (1970).
- [25] R. J. Peláez, C. Blondel, C. Delsart, and C. Drag, *J. Phys. B: At., Mol. Opt. Phys.* **42**, 125001 (2009).
- [26] X. Yuan and A. S. Pereira Gomes, *J. Chem. Phys.* **157**, 074313 (2022).
- [27] J. V. Pototschnig, K. G. Dyall, L. Visscher, and A. S. P. Gomes, *Phys. Chem. Chem. Phys.* **23**, 22330 (2021).
- [28] M. Denis, M. S. Nørby, H. J. A. Jensen, A. S. P. Gomes, M. K. Nayak, S. Knecht, and T. Fleig, *New J. Phys.* **17**, 043005 (2015).